Applied Surface Science 515 (2020) 145985

Contents lists available at ScienceDirect

Applied Surface Science

journal homepage: www.elsevier.com/locate/apsusc

Full Length Article

Reverse water-gas shift chemistry inside a supersonic molecular beam nozzle

Rebecca S. Thompson, Grant G. Langlois, Wenxin Li, Michelle R. Brann, S.J. Sibener*

The James Franck Institute and Department of Chemistry, The University of Chicago, 929 E 57th Street, Chicago, IL 60637, United States

ARTICLE INFO

Keywords:
Reverse water-gas shift reaction
Surface catalysis
Supersonic expansion molecular beam
CO_2 conversion
CO production
Stainless steel

ABSTRACT

Resistive heating of the metal surface of a supersonic molecular beam nozzle is shown to be very effective in converting CO_2 diluted in H_2 to CO and H_2O *via* the reverse water–gas shift (RWGS) reaction at temperatures that preclude simple pyrolysis. The conversion of CO_2 to CO, referred to herein as "RWGS yield," exceeds 80% at nozzle temperature above 1000 K, with a detectable methane byproduct. The stainless-steel surface of the nozzle appears to facilitate the reaction as a heterogeneous catalyst. Reaction yield is observed to increase with nozzle temperature and, when the gas mixture contains a significant excess of H_2, decrease with increasing in nozzle stagnation pressure. The inverse dependence of the reaction on stagnation pressure is used to propose a reaction mechanism. Additional kinetic control over the mechanism is afforded by adjusting reactant partial pressures and residence times inside the nozzle reactor, highlighting this method's utility in screening heterogeneous catalysis reactions with fine control over mass flow rates, pressure, and temperature. The results of this study, therefore, present a route to efficient, high pressure, inline catalysis as well as a method to rapidly assess the viability of new catalysts in development.

1. Introduction

Thermodynamic equilibrium of the system containing carbon dioxide, hydrogen, water vapor, and carbon monoxide is at the center of mass production of high-demand chemicals including ammonia and methanol [1,2]. The direct reaction of carbon dioxide with hydrogen is an endothermic reaction known as the reverse water–gas shift reaction (RWGS). The RWGS reaction is endothermic by 41 kJ mol^{-1}, expressed by the equation [3]:

$$H_2 + CO_2 \rightleftharpoons CO + H_2O \quad (1)$$

This reaction has not attracted as much attention as its forward-direction counterpart, but the RWGS reaction, particularly at high temperatures, can often play a role in the overall observed kinetics. RWGS conversion is typically below 50% under typical experimental conditions [3–7] and extraneous alcohol or hydrocarbon byproducts often accompany the desired products. These byproducts come from Fischer-Tropsch reactions branching from intermediate steps in the RWGS reaction [8,9].

Two general methods are employed for the water-gas shift reactions: high-temperature pyrolysis and heterogeneous catalysis [4,5,10–13]. The former typically requires temperatures above 1000 K to overcome the energetic barrier. The latter is generally efficient for a variety of metal and metal-oxide catalysts [12]. The experimental conditions in the current study produce a facile route for high conversion yield of CO_2 to CO as measured by time-of-flight mass spectrometry (TOF-MS). Unique to this study is the use of a supersonic molecular beam as the reactor. The nozzle's stainless-steel surface serves as the heterogeneous catalyst and the products are sampled via TOF-MS after exiting the beam's hot nozzle.

This beam-as-reactor method has been used to generate radical reactants via pyrolytic unimolecular dissociation [14,15] as well as to study catalytic hydrocarbon formation. Shebaro *et al.* reported large hydrocarbons, including benzene, in the product stream of a supersonic beam of ethane at elevated nozzle temperatures [16,17]. Romm *et al.* expanded upon this work; they elucidated the interplay of kinetic and thermodynamic control of methane pyrolysis in a heated nozzle by identifying changes in products under different flow conditions [18,19]. In addition to the catalytic role of the nozzle material, relatively short nozzle residence times and the rapid cooling of reaction products in the expansion lead to a unique reaction environment in which traditional steady-state equilibrium assumptions do not apply.

In the current study, we use a similar setup to sample the RWGS reaction products. Unlike prior work sampling reaction products via TOF-MS following desorption from a surface, we feed the reactive mixture of H_2 and CO_2 into the hot stainless-steel nozzle of the supersonic beam source, which serves as the catalytic site [20–23]. Downstream, with a mass spectrometer along the direct line-of-sight from the

* Corresponding author.
E-mail address: s-sibener@uchicago.edu (S.J. Sibener).

https://doi.org/10.1016/j.apsusc.2020.145985
Received 18 January 2020; Received in revised form 27 February 2020; Accepted 5 March 2020
Available online 06 March 2020

differentially pumped beam, we measure conversion yields of CO_2 to CO of ~50% by 800 K; the yield is above 80% by 1000 K. We discuss the reaction mechanism and examine the extent of extraneous Fischer-Tropsch reactivity under these conditions. We also determine the extent of kinetic control over the product stream afforded by our experimental conditions.

2. Experimental

2.1. Supersonic beam source

Experiments were conducted using a triply-differentially pumped supersonic beamline, described previously [24]. A gas mixture of 10%, 50%, or 88% CO_2 diluted in H_2 flows into a 316 stainless-steel nozzle gland fitted with a 20 μm diameter pinhole made of molybdenum. Platinum pinholes were also tested to confirm that the pinhole material had no impact on reaction yield. Coiled along the outer length of the gland is resistively-heated wire (Thermocoax). A thin tantalum sheet is secured around the wire coil and gland with copper wire; this construction promotes efficient and even heating along the length of the gland. The temperature is held constant with an Omega CN76000 temperature controller, monitored by a Type-K thermocouple spot-welded onto the tip of the nozzle ~2–3 mm from the pinhole. With this setup, reactivity was studied using nozzle temperatures up to 1025 K and stagnation pressures between 600 and 3100 kPa (90–450 psi). The beam was always equilibrated for at least 30 min prior to data acquisition after changing either the nozzle temperature or stagnation pressure.

The supersonic beam is modulated by a chopper wheel located in the first differential chamber of the beamline. The beam is square-wave (SQW) modulated at 100 Hz with a 50% duty cycle. Relative product intensities are detected downstream by an inline quadrupole mass spectrometer located in the adjacent ultra-high vacuum (UHV) chamber open to the beamline.

2.2. Calculating RWGS yield

Quantifying CO_2 to CO conversion involves comparison of SQW modulated data at $m/z = 28$ and $m/z = 44$ at room and elevated temperatures. Total intensity at any given m/z value is derived from the difference in the sums of four consecutive 200 μs bins with the beam passing and blocked by the chopper wheel. At room temperature, the CO/CO_2 intensity ratio is not zero due to electron dissociative detachment of CO_2. Thus, the signals obtained at $m/z = 28$ and $m/z = 44$ with the nozzle at room temperature are:

$$I_{28} = CQ_{28}[N_{CO_2}\sigma_D] \tag{2}$$

$$I_{44} = CQ_{44}[N_{CO_2}\sigma_{CO_2}] \tag{3}$$

And the intensity ratio at room temperature (with no reaction), η_L, is therefore:

$$\eta_L = \frac{I_{28}}{I_{44}} = \frac{CQ_{28}[N_{CO_2}\sigma_D]}{CQ_{44}[N_{CO_2}\sigma_{CO_2}]} = \frac{Q_{28}}{Q_{44}}\frac{\sigma_D}{\sigma_{CO_2}} \tag{4}$$

N_{CO_2} and N_{CO} are the number densities of CO_2 and CO, Q_{44} and Q_{28} are the quadrupole transmission coefficients at $m/z = 44$ and $m/z = 28$, and C is an empirical constant related to our particular instrument, and is canceled out in Eq. (4). For ionization with 100 eV electrons, the quoted cross-sections are [25]:

$$CO_2 + e^- \xrightarrow{\sigma_D} CO^+ + O + 2e^-;\ \sigma_D = 0.389\text{Å}^2 \tag{5}$$

$$CO_2 + e^- \xrightarrow{\sigma_{CO_2}} CO_2^+ + 2e^-;\ \sigma_{CO_2} = 2.25\text{Å}^2 \tag{6}$$

As the nozzle temperature is raised and the RWGS reaction occurs, the signal at $m/z = 28$ now has contributions from CO_2 left in the product stream (Eq. (5)) and the newly-formed CO:

$$I_{28} = CQ_{28}[N_{CO_2}\sigma_D] + CQ_{28}[N_{CO}\sigma_{CO}] \tag{7}$$

The intensity ratio during catalysis, η_H, is now:

$$\eta_H = \frac{I_{28}}{I_{44}} = \frac{CQ_{28}[N_{CO_2}\sigma_D] + CQ_{28}[N_{CO}\sigma_{CO}]}{CQ_{44}[N_{CO_2}\sigma_{CO_2}]} = \frac{Q_{28}}{Q_{44}}\left(\frac{\sigma_D}{\sigma_{CO_2}} + \frac{N_{CO}}{N_{CO_2}}\frac{\sigma_{CO}}{\sigma_{CO_2}}\right) \tag{8}$$

The new ionization cross-section introduced in Eq. (7) is simply [26]:

$$CO + e^- \xrightarrow{\sigma_{CO}} CO^+ + 2e^-;\ \sigma_{CO} = 1.82\text{Å}^2 \tag{9}$$

Dividing Eq. (8) by Eq. (4) and solving for the CO to CO_2 number density ratio, R, eliminates the transmission coefficients from consideration:

$$R = \frac{N_{CO}}{N_{CO_2}} = \left(\frac{\eta_H}{\eta_L} - 1\right)\frac{\sigma_D}{\sigma_{CO}} \tag{10}$$

The fraction of CO_2 converted to CO, defined here as the RWGS yield, is a function of R defined in Eq. (10):

$$\frac{N_{CO}}{N_{CO} + N_{CO_2}} = \frac{R}{R+1} \tag{11}$$

3. Results and discussion

3.1. Evidence for RWGS reaction

Reactivity is evident in comparing representative SQW modulated data in Fig. 1 obtained from a supersonic beam with a stagnation pressure of 1725 kPa. Near room temperature, when no reaction is expected, there are the anticipated signals at $m/z = 28$ and $m/z = 44$, attributed entirely to the ionization and dissociative detachment of CO_2 in the beam (Eqs. (5) and (6)). Upon heating the nozzle to 800 K, however, the CO_2 intensity drops significantly, while the signal at $m/z = 28$ increases. We also observe new signal intensity at $m/z = 18$, due to H_2O formation in the nozzle. This indicates significant RWGS reactivity.

Though the RWGS reaction is the primary mechanism, we also observe some evidence that secondary reaction channels are active at the highest temperatures studied. For example, we see significant signal

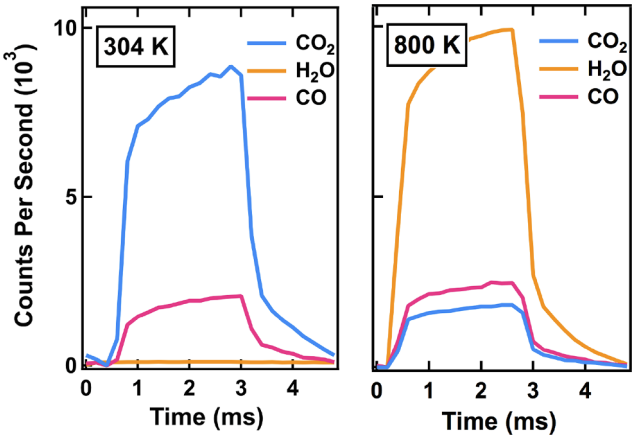

Fig. 1. Representative square wave TOF-MS signals at $m/z = 18$ (H_2O, yellow), 28 (CO, pink), and 44 (CO_2, blue). At room temperature (left), the only contribution to signal intensity at $m/z = 28$ is the dissociative ionization of CO_2 (Eq. (5)). Upon heating the nozzle to 800 K (right), RWGS reactivity is evidenced by a dramatic increase in the ratio of CO to CO_2, as well as new signal intensity at $m/z = 18$ (attributed to H_2O formation). These data were collected using the 10% CO_2 gas mixture at 1725 kPa. (For interpretation of the references to color in this figure legend, the reader is referred to the web version of this article.)

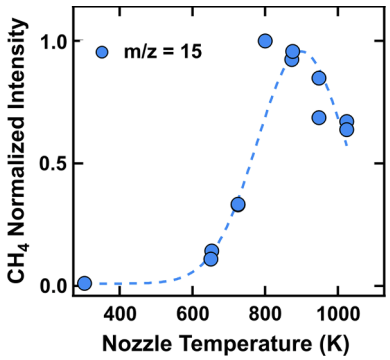

Fig. 2. TOF-MS signal at $m/z = 15$ is observed at high temperatures in the nozzle, likely corresponding to the generation of methane. Above ~800 K, the relative amount of methane in the product stream decreases, signaling loss of methane likely due to coupling Fischer-Tropsch processes. These data were collected using the 10% CO_2 gas mixture at 1725 kPa. Dotted line is drawn to guide the eye.

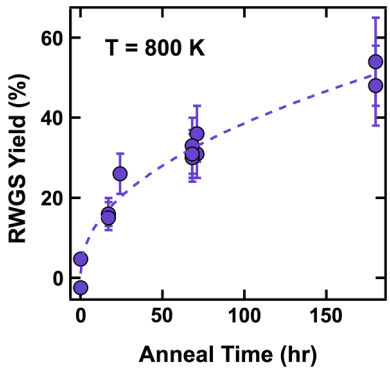

Fig. 3. RWGS yield as a function of vacuum annealing treatment of nozzle. The 316 stainless-steel nozzle does not show appreciable catalytic activity of any kind until it has been annealed at 800 K under vacuum. The RWGS yield (for the 10% CO_2 gas mixture at a stagnation pressure of 1725 kPa) reaches 50% after roughly 180 h of vacuum annealing at 800 K. Dotted line drawn to guide the eye. Error bars represent one standard deviation.

intensity at $m/z = 15$ that cannot be attributed to the initial gas mixture. Shown in Fig. 2, the normalized intensity at $m/z = 15$ increases with nozzle temperature, peaking near 800 K before starting to decrease thereafter. Moreover, after extended use at the highest temperatures studied (weeks of operation with consistent daily use), the nozzle eventually clogs with soot (or coke) and must be taken apart and sonicated to continue.

Under our reaction conditions, both Fischer-Tropsch or CO_2 methanation (Sabatier) reactions are possible explanations for this observation [27,28]. In monitoring the product stream, however, we do not see any evidence of Fischer-Tropsch byproducts such as formaldehyde and ethanol ($m/z = 29$ and 31, respectively) or other large, unsaturated hydrocarbons. This makes sense, as significant Fischer-Tropsch reactivity would necessarily consume any CO generated by the RWGS reaction. Any trace Fischer-Tropsch reactivity that is taking place is likely, under our conditions, to have high methane selectivity anyway due to our high temperatures and H_2/CO ratios, as well as the nozzle's role as an un-promoted iron-based catalyst [29–31]. It is possible that the decrease in methane signal above 800 K is due to some methane coupling in the nozzle [16–19], contributing to the eventual clogging, but in general it appears that the most significant secondary reaction is simply the production of methane or other surface carbide species directly from CO_2 and H_2 [32–34]. We also note that these observations align well with previous reports from Romm *et al.*, which demonstrated that metal nozzles were more prone to contamination with surface carbide species and correspondingly less active in the conversion of methane to higher hydrocarbons [18,19].

Notably, the stainless-steel nozzle *does not* exhibit considerable RWGS catalytic activity until it has been thermally annealed under vacuum for dozens of hours. Fig. 3 demonstrates the effect of vacuum annealing of the nozzle at 800 K on the RWGS yield. The yield, as measured using a nozzle temperature of 800 K and stagnation pressure of 1725 kPa, is essentially zero with no treatment, and has leveled off near ~50% after 180 h of vacuum annealing at 800 K. This observation can be rationalized by considering the stainless steel surface. As produced, the passive property of stainless steel derives from iron and chromium oxide surface layers. Annealing under vacuum, however, can significantly alter the composition of the surface. At modest vacuum annealing temperatures, (500–800 K), the surface sees a decrease in graphitic and hydrocarbon contamination as well as an increase in chromium content [35–39]. Both of these effects may be crucial in maintaining a high number of active sites on the catalytic substrate. Mixed iron and chromium oxides are common catalysts for both the forward and reverse water-gas shift reactions [1,12,40,41]. Many researchers have also highlighted the significant role chromium plays in stabilizing the surface and preventing sintering [1,40,42,43]. Though the prevention of sintering may be more directly relevant to powdered catalytic systems, it is clear that given the vacuum annealing time required to achieve significant catalytic activity, chromium enrichment, as cited above, is an important effect and directly enables the high-yield RWGS reaction.

At constant stagnation pressure, RWGS yield is obtained only at high nozzle temperatures. This is expected from the reaction's endothermicity. Shown in Fig. 4, once the nozzle temperature exceeds 650 K, conversion of CO_2 to CO is observed, and the total conversion increases with increasing temperature throughout the entire range studied in this work. While hydrocarbons are evidently produced to some extent, the total conversion of CO_2 to CO is very high above 800 K, reaching above 80% by 1025 K. It is worth noting, however, that the yield appears to plateau at the lowest and highest temperatures studied. The fact that there is no significant yield below 650 K suggests a thermally activated process; likely the dissociation of H_2 [44–47]. It is less likely that this activation arises from a sudden freeing of surface active sites for dissociative adsorption; CO and CO_2 are present in such dilute amounts, and their desorption from Fe-based surfaces typically occurs at slightly higher temperatures [48–51]. At the highest temperatures studied, on the other hand, increases in reaction yield appear to slow. Again, this behavior may be understood by considering the composition of the stainless steel interface at these temperatures. While modest annealing temperatures lead to chromium *enrichment* as discussed above, temperatures above 1000–1100 K lead to a significant *depletion* in surface chromium levels [36,37,52–54]. A loss of active sites, therefore, may explain why peak reactive yields do not exceed 85%.

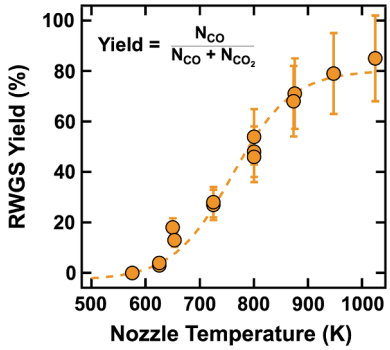

Fig. 4. RWGS yield increases as a function of nozzle temperature. Given the endothermic nature of the reaction, increasing the nozzle temperature leads to a higher RWGS yield for the 10% CO_2 gas mixture at a constant stagnation pressure of 1725 kPa. Dotted line drawn to guide the eye. Error bars represent one standard deviation.

3.2. Reaction mechanism and kinetic control

The mechanisms of RWGS reactions have been studied both in the gas phase and over catalysts [4,6,7,10,12]. Several early investigations suggested surface-mediated processes, with the mechanism broadly classified as either regenerative or associative [4,7]. Reported mechanisms are frequently dependent upon catalyst composition and reaction temperature, and considerable dispute remains in mechanistic studies [2,4,28]. In light of our current results and utilizing some key assumptions, we attempt to describe the RWGS reaction mechanism taking place within our nozzle. High-temperature pyrolysis would require temperatures higher than those studied here, so we can assert that a surface-specific process is taking place [8,10]. Several authors have studied RWGS reactivity under similar temperature and pressure conditions with inert quartz reactors and conversion was typically less than 0.1% [3,6]. Bustamante and co-workers compared yields for quartz and metallic chambers; they found a dramatic increase in catalytic activity with a metallic surface, resulting in conversion rates of up to 55% at 1173 K under ambient pressure [3,55]. They concluded that the metal surfaces of the reactor directly catalyzed the reaction. Similarly, surface-facilitated reactions utilizing supersonic beams have also been demonstrated in other studies. For example, Romm *et al.* reported close to 100% conversion of ethane to heavier hydrocarbons in a supersonic nozzle beam; their proposed mechanism relied heavily on surface-mediated hydrogen abstraction processes [18,19].

Based on the above discussion, we postulate one possible mechanism (Scheme 1), wherein the (*) subscript denotes a surface site and X* is a surface-adsorbed X species. This mechanism is based on the frequently-cited redox mechanisms for high-temperature WGS catalysis in both the forward and reverse directions [1,7,41,56]. Given the large excess of H_2 in our reaction mixture and the relatively facile dissociation on steel, we assume that the limiting step under our reaction conditions is the dissociation of CO_2. Therefore, the overall rate can be represented by:

$$\text{Rate} = \frac{dP_{CO}}{dt} = k_3 \theta_{CO_2*} \theta_* \tag{12}$$

Additionally, the fractional coverage of adsorbed CO_2 (θ_{CO_2*}) can be determined from the equilibrium in step 2:

$$\theta_{CO_2*} = K_2 P_{CO_2} \theta_* \tag{13}$$

By combining these two equations and assuming that hydrogen coverage on the surface remains approximately constant and CO_2 is competing for the remaining sites, we can derive a rate expression:

$$\text{Rate} = \frac{dP_{CO}}{dt} = \frac{k_3 K_2 P_{CO_2}}{(1 + K_2 P_{CO_2})^2} \tag{14}$$

Though we do not measure rates directly in this study, we can approximate them by recognizing that nozzle residence times do not change as a function of stagnation pressure [57]. Therefore, measuring yield as a function of CO_2 partial pressure allows us to partially assess the feasibility of this rate law. These results are shown in Fig. 5, where RWGS reaction yield is observed to decrease as a function of CO_2 partial pressure. Eq. (14) is a good fit for the data, but our limited pressure range makes it difficult to say with certainty that this predicted rate law

$$\begin{aligned}
&(1) && H_{2(g)} + 2* \rightleftharpoons 2H* \\
&(2) && CO_{2(g)} + * \rightleftharpoons CO_2* \\
&(3) && CO_2* + * \rightarrow CO* + O* \\
&(4) && O* + 2H* \rightleftharpoons H_2O* + 2* \\
&(5) && CO* \rightarrow CO_{(g)} + * \\
&(6) && H_2O* \rightarrow H_2O_{(g)} + *
\end{aligned}$$

Scheme 1. Proposed mechanism for high pressure, high temperature RWGS reaction for a 10% CO_2 in H_2 gas mixture in a stainless steel beam nozzle reactor.

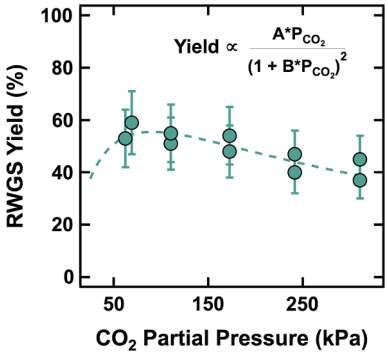

Fig. 5. RWGS yield decreases as a function of CO_2 partial pressure (10% CO_2 in H_2 gas mixture) at a constant nozzle temperature of 800 K. Dashed line is a fit of the data to Eq. (14), which is a proposed mechanism for the reaction assuming CO_2 dissociation on the metal surface is the rate-limiting step.

completely describes the reaction. It is clear, however, that there is a small negative power dependence for the rate on CO_2 partial pressure. This has been observed occasionally in previous studies [1,58], but we note that it is common for WGS power rate laws to change significantly across different catalyst systems, temperatures, and relative reactant pressures. In other words, Eq. (14) may only be appropriate for the data in this particular pressure, temperature, and reaction mixture regime.

When considering the RWGS mechanism, we also note the interplay between heterogenous catalysis and the unique role of the supersonic expansion and nozzle geometry. The lineage of this discussion stretches back to the cited work by the Herschbach and Somorjai research groups [16–19]. As discussed by Shebaro *et. al.* [16,17], the metal nozzle plays a clear catalytic role, likely involving the dissociation of H_2 and CO_2 in this case. Under our high pressure conditions, these radical and surface-bound species react rapidly to form RWGS products. Gas phase products are then quickly quenched by the expansion and exit the beam, circumventing further degradation and reaction on the hot nozzle surface [18,19]. Residence times in the current study are on the order of 10–100 ms, which provides enough time for the reaction to take place, while also cooling and removing the products (specifically CO) before they can continue to react significantly to form heavier hydrocarbons via Fischer-Tropsch synthesis [59]. It appears, therefore, that the mechanism reported here depends on both the nature of the supersonic expansion (control of residence times and rapid removal of reaction products) and the catalytically-active metal nozzle.

The challenge of establishing a universal mechanism for this reaction is highlighted when we consider that the dissociation of H_2 (Scheme 1, step 1) can also be a key step, depending on reaction conditions. In the 10% mixture, H_2 drastically outnumbers the CO_2. Given the facile splitting of H_2 on the stainless steel, we assume that the oxygen atoms left from the dissociative chemisorption of CO_2 can generate water immediately (Scheme 1, step 4). Strengthening this argument are a series of experiments we performed with two additional mixtures of CO_2 and H_2: 50% and 88% CO_2 diluted in H_2. The results in Fig. 6 show that the RWGS yields for the less dilute mixtures are significantly lower than the 10% mixture over the same high temperature range. Though the yield may be decreasing in part due to the increase in CO_2 partial pressures for the 50% and 88% mixture (as discussed for Fig. 5), it also appears that excess H_2 is critical in facilitating high yields. Without an excess of H_2 in the feed gas, the rate-limiting step may change, leading to a slowdown in CO production; though CO_2 may be able to adsorb more readily, the number of hydrogen atoms on the surface available for reaction will also decrease.

4. Conclusions

Utilizing a supersonic expansion from a heated stainless steel nozzle, we demonstrate selective CO_2 reduction to CO by H_2 involved in

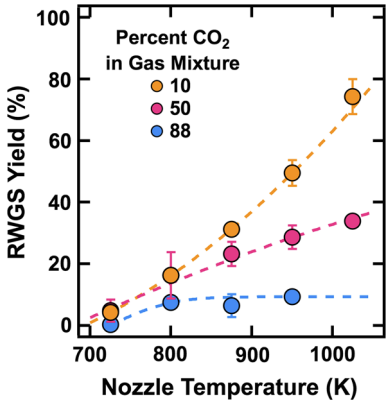

Fig. 6. Representative RWGS yields for various mixtures of CO_2 and H_2 at varying temperatures and constant stagnation pressure (1725 kPa). Without an excess of H_2 in the feed gas, the reduction of CO_2 to CO relative to the dilute 10% mixture plummets at high temperature. Dotted lines drawn to guide the eye.

the RWGS reaction. This reaction exhibits conversion yields above 80% at nozzle temperatures above 1000 K. The yield of the reaction increases as nozzle temperature increases and decreases with higher stagnation pressure (and CO_2 partial pressure). The stainless-steel surface was found to serve as a heterogeneous catalyst for the reaction. A small amount of methane is formed as a byproduct, and may be further converted to heavier hydrocarbons when the nozzle temperature is above 800 K.

We propose a mechanism for the reaction under our conditions and probe its applicability through precise control of reaction mixture, residence time in the nozzle reactor, and nozzle temperature. The nozzle reaction chamber is a unique environment in which heterogenous catalysis on the nozzle surface is coupled with rapid cooling of reaction products in the supersonic expansion. Future work may expand this investigation to include the impact of different nozzle materials and pinhole sizes on mechanism and total reaction yield. In addition to characterizing the RWGS reaction catalyzed on stainless steel under high pressure conditions, this supersonic expansion technique also provides broad opportunities to screen various catalytic reactions under variable pressure and temperature conditions. It is feasible for this technique to facilitate such reactions with surface-generated gas-phase radicals, followed by rapid desorption and cooling of the intermediate products. This method, therefore, affords a rapid, quantitative, and comprehensive screening ansatz of catalytic efficiency.

Author contributions

Authors R.S.T., G.G.L., W.L., M.R.B, and S.J.S. all participated in formal analysis, data curation, investigation, and methodolgy. R.S.T. and G.G.L. were responsible for writing - original draft. R.S.T., G.G.L, M.R.B., and S.J.S. were responsible for writing - review & editing. S.J.S. was additionally responsible for science conceptualization, resources, supervision, and funding acquisition.

Declaration of Competing Interest

The authors declare that they have no known competing financial interests or personal relationships that could have appeared to influence the work reported in this paper.

Acknowledgements

This work was supported by the National Science Foundation [Grant No. CHE-1900188]. Additional support was provided by the NSF-Materials Research Science and Engineering Center at The University of Chicago [Grant No. NSF-DMR-14-20709]. Conversations with Kevin D. Gibson are also gratefully acknowledged.

References

[1] C. Ratnasamy, J.P. Wagner, Water gas shift catalysis, Catal. Rev. 51 (2009) 325–440.
[2] R. Smith, M. Loganathan, M. Shantha, A review of the water gas shift reaction kinetics, Int. J. Chem. React. Eng. 8 (2010) 1–32.
[3] F. Bustamante, R. Enick, K. Rothenberger, Kinetic study of the reverse water gas shift reaction in high-temperature, high pressure homogeneous systems, Fuel Chem. Div. 47 (2002) 663–664.
[4] D.S. Newsome, The water-gas shift reaction, Catal. Rev. 21 (1980) 275–318.
[5] D.J. Pettigrew, D.L. Trimm, N.W. Cant, The effects of rare earth oxides on the reverse water-gas shift reaction on palladium/alumina, Catal. Lett. 28 (1994) 313–319.
[6] G. Tingey, Kinetics of water-gas equilibrium reaction, J. Phys. Chem. 70 (1966) 1406–1412.
[7] M.J.L. Ginés, A.J. Marchi, C.R. Apesteguía, Kinetic study of the reverse water-gas shift reaction over $CuO/ZnO/Al_2O_3$ catalysts, Appl. Catal. A Gen. 154 (1997) 155–171.
[8] G. Weatherbee, C. Bartholomew, Hydrogenation of CO_2 on group VIII metals: IV. Specific activities and selectivities of silica-supported Co, Fe, and Ru, J. Catal. 87 (1984) 352–362.
[9] C. Rofer-DePoorter, Comprehensive mechanism for the fischer-tropsch synthesis, Chem. Rev. 81 (1981) 446–474.
[10] B. Bradford, The water-gas reaction in low-pressure explosions, J. Chem. Soc. 1557–1563 (1933).
[11] G. Chinchen, M. Spencer, K. Waugh, Promotion of methanol synthesis and the water-gas shift reactions by adsorbed oxygen on supported copper catalysts, J. Chem. Soc. 83 (1987) 2193–2212.
[12] M.S. Spencer, On the activation energies of the forward and reverse water-gas shift reaction, Catal. Lett. 32 (1995) 9–13.
[13] R. Koeppel, A. Baiker, A. Wokaun, Copper/zirconia catalysts for the synthesis of methanol from carbon dioxide: influence of preparation variables on structural and catalytic properties of catalysts, Appl. Catal. A Gen. 84 (1992) 77–102.
[14] D.W. Kohn, H. Clauberg, P. Chen, Flash pyrolysis nozzle for generation of radicals in a supersonic jet expansion, Rev. Sci. Instrum. 63 (1992) 4003–4005.
[15] X. Zhang, A.V. Friderichsen, S. Nandi, G.B. Ellison, D.E. David, J.T. McKinnon, T.G. Lindeman, D.C. Dayton, M.R. Nimlos, Intense, hyperthermal source of organic radicals for matrix-isolation spectroscopy, Rev. Sci. Instrum. 74 (2003) 3077–3086.
[16] L. Shebaro, S. Bhalotra, D. Herschbach, Molecular beam chemistry: formation of benzene and other higher hydrocarbons from small alkanes and alkenes in a catalytic supersonic nozzle, J. Phys. Chem. A 101 (1997) 6775–6780.
[17] L. Shebaro, B. Abbott, T. Hong, A. Slenczka, B. Friedrich, D. Herschbach, Facile production of higher hydrocarbons from ethane in a catalytic supersonic nozzle, Chem. Phys. Lett. 271 (1997) 73–78.
[18] L. Romm, G. Somorjai, High-temperature short-contact-time supersonic nozzle chemistry of light aliphatic hydrocarbons, Top. Catal. 30 (2002) 53–62.
[19] L. Romm, Y. Kim, G. Somorjai, Methane chemistry in the hot supersonic nozzle, J. Phys. Chem. A 105 (2001) 7025–7030.
[20] J.I. Colonell, K.D. Gibson, S.J. Sibener, Carbon monoxide oxidation on Rh(111): velocity and angular distributions of the CO_2 product, J. Chem. Phys. 103 (1995) 6677–6690.
[21] K.D. Gibson, J.I. Colonell, S.J. Sibener, Oxidation of H on Rh(111): H_2O product velocity and angular distributions, J. Chem. Phys. 103 (1995) 6735–6739.
[22] L.S. Brown, S.J. Sibener, A molecular beam scattering investigation of the oxidation of CO on Rh(111). II. Angular and velocity distributions of the CO_2 product, J. Chem. Phys. 90 (1989) 2807–2815.
[23] L.S. Brown, S.J. Sibener, A Molecular beam scattering investigation of the oxidation of CO on Rh(111). I. Kinetics and mechanism, J. Chem. Phys. 89 (1988) 1163–1169.
[24] G.G. Langlois, W. Li, K.D. Gibson, S.J. Sibener, Capture of hyperthermal CO_2 by amorphous water ice via molecular, Embedding (2015).
[25] Y. Itikawa, Cross sections for electron collisions with carbon dioxide, J. Phys. Chem. Ref. Data 31 (2002) 749–767.
[26] C. Tian, C.R. Vidal, Cross sections of the electron impact dissociative ionization of CO, CH_4 and C_2H_2, J. Phys. B At. Mol. Opt. Phys. 31 (1998) 895–909.
[27] V. Ponec, Some aspects of the mechanism of methanation and Fischer-Tropsch synthesis, Catal. Rev. 18 (1978) 151–171.
[28] W. Wang, S. Wang, X. Ma, J. Gong, Recent advances in catalytic hydrogenation of carbon dioxide, Chem. Soc. Rev. 40 (2011) 3703–3722.
[29] J. Yang, W. Ma, D. Chen, A. Holmen, B.H. Davis, Fischer-Tropsch synthesis: a review of the effect of CO conversion on methane selectivity, Appl. Catal. A Gen. 470 (2014) 250–260.
[30] W. Ma, W.D. Shafer, G. Jacobs, J. Yang, D.E. Sparks, H.H. Hamdeh, B.H. Davis, Fischer-Tropsch synthesis: effect of CO conversion on CH_4 and oxygenate selectivities over precipitated Fe-K catalysts, Appl. Catal. A Gen. 560 (2018) 144–152.
[31] H. Matsumoto, C.O. Bennett, The transient method applied to the methanation and Fischer-Tropsch reactions over a fused iron catalyst, J. Catal. 53 (1978) 331–344.
[32] G.A. Mills, F.W. Steffgen, Catalytic methanation, Catal. Rev. 8 (1974) 159–210.
[33] J.W. Niemantsverdriet, A.M. van der Kraan, On the time-dependent behavior of iron catalysts in Fischer-Tropsch synthesis, J. Catal. 72 (1981) 385–388.
[34] C.V. Miguel, M.A. Soria, A. Mendes, L.M. Madeira, Direct CO_2 hydrogenation to methane or methanol from post-combustion exhaust streams - a thermodynamic

study, J. Nat. Gas Sci. Eng. 22 (2015) 1–8.
[35] R.O. Adams, A review of the stainless steel surface, J. Vac. Sci. Technol. A Vacuum, Surfaces, Film. 1 (1983) 12–18.
[36] G. Bombara, A. Alderisio, U. Bernabai, M. Cavallini, The effects of heating in a vacuum on the surface properties of a low chromium stainless steel, Surf. Technol. 14 (1981) 17–23.
[37] R. Wild, Vacuum annealing of stainless steel at temperatures between 770 and 1470K, Corros. Sci. 14 (1974) 575–586.
[38] R. Park, J. Houston, D. Schreiner, Chromium depletion of vacuum annealed stainless steel surfaces, J. Vac. Sci. 9 (1972) 1023–1027.
[39] G. Hultquist, C. Leygraf, Highly protective films on stainless steels, Mater. Sci. Eng. 42 (1980) 199–206.
[40] Y. Lei, N.W. Cant, D.L. Trimm, Kinetics of the water-gas shift reaction over a rhodium-promoted iron-chromium oxide catalyst, Chem. Eng. J. 114 (2005) 81–85.
[41] Y.A. Daza, J.N. Kuhn, CO_2 conversion by reverse water gas shift catalysis: comparison of catalysts, mechanisms and their consequences for CO_2 conversion to liquid fuels, RSC Adv. 6 (2016) 49675–49691.
[42] C.J. Keturakis, M. Zhu, E.K. Gibson, M. Daturi, F. Tao, A.I. Frenkel, I.E. Wachs, Dynamics of CrO_3 –Fe_2O_3 catalysts during the high-temperature water-gas shift reaction: molecular structures and reactivity, ACS Catal. 6 (2016) 4786–4798.
[43] D.-W. Lee, M.S. Lee, J.Y. Lee, S. Kim, H.-J. Eom, D.J. Moon, K.-Y. Lee, The review of Cr-free Fe-based catalysts for high-temperature water-gas shift reactions, Catal. Today 210 (2013) 2–9.
[44] T.J. Marrow, P.J. Cotterill, J.E. King, Temperature effects on the mechanism of time independent hydrogen assisted fatigue crack propagation in steels, Acta Metall. Mater. 40 (1992) 2059–2068.
[45] R.W. Pasco, P.J. Ficalora, The adsorption of hydrogen on iron; A Surface orbital modified occupancy — bond energy bond order calculation, Surf. Sci. 134 (1983) 476–498.
[46] C. Zou, A.C.T. van Duin, D.C. Sorescu, Theoretical investigation of hydrogen adsorption and dissociation on iron and iron carbide surfaces using the ReaxFF reactive force field method, Top. Catal. 55 (2012) 391–401.
[47] R.A. Oriani, Hydrogen embrittlement of steels, Annu. Rev. Mater. Sci. 8 (1978) 327–357.
[48] K. Yoshida, G.A. Somorjai, The chemisorption of CO, CO_2, C_2H_2, C_2H_4, H_2 and NH_3 on the clean Fe(100) and (111) crystal surfaces, Surf. Sci. 75 (1978) 46–60.
[49] D.W. Moon, S.L. Bernasek, D.J. Dwyer, J.L. Gland, Observation of an unusually low CO stretching frequency on Fe(100), J. Am. Chem. Soc. 107 (1985) 4363–4364.
[50] D.W. Moon, D.J. Dwyer, S.L. Bernasek, Adsorption of CO on the clean and sulfur modified Fe(100) surface, Surf. Sci. 163 (1985) 215–229.
[51] H.J. Freund, M.W. Roberts, Surface chemistry of carbon dioxide, Surf. Sci. Rep. 25 (1996) 225–273.
[52] R.C. Lobb, H.E. Evans, An evaluation of the effect of surface chromium concentration on the oxidation of a stainless steel, Corros. Sci. 23 (1983) 55–73.
[53] J.C. Killeen, A.F. Smith, R.K. Wild, Chromium depletion profiles after preferential removal of chromium from alloys, Corros. Sci. 16 (1976) 551–559.
[54] R.G. Musket, W. Bauer, Surface characterization of stainless steel using proton-induced X rays, Appl. Phys. Lett. 20 (1972) 411–413.
[55] F. Bustamante, R.M. Enick, A.V. Cugini, R.P. Killmeyer, B.H. Howard, K.S. Rothenberger, M.V. Ciocco, B.D. Morreale, S. Chattopadhyay, S. Shi, High-temperature kinetics of the homogeneous reverse water-gas shift reaction, AIChE J. 50 (2004) 1028–1041.
[56] J.A. Loiland, M.J. Wulfers, N.S. Marinkovic, R.F. Lobo, Fe/γ-Al_2O_3 and Fe–K/γ-Al_2O_3 as reverse water-gas shift catalysts, Catal. Sci. Technol. 6 (2016) 5267–5279.
[57] G. Scoles, Free jet sources, in: D. Bassi, U. Buck, D. Laine (Eds.), Atomic and Molecular Beam Methods, Vol. 1 Oxford University Press, New York, 1988, pp. 14–53.
[58] M. Zhu, I.E. Wachs, Iron-Based Catalysts for the high-temperature water-gas shift (HT-WGS) Reaction: a review, ACS Catal. 6 (2016) 722–732.
[59] L. Torrente-Murciano, D. Mattia, M.D. Jones, P.K. Plucinski, Formation of hydrocarbons via CO_2 hydrogenation - a thermodynamic study, J. CO2 Util. 6 (2014) 34–39.